

University of Wollongong
Research Online

Faculty of Engineering - Papers (Archive)

Faculty of Engineering and Information
Sciences

1-1-2008

Dependency of recrystallization mechanism to the initial grain size

A Dehghan-Manshadi
University of Wollongong, alidm@uow.edu.au

P D. Hodgson
Deakin University

Follow this and additional works at: <https://ro.uow.edu.au/engpapers>

 Part of the [Engineering Commons](#)

<https://ro.uow.edu.au/engpapers/971>

Recommended Citation

Dehghan-Manshadi, A and Hodgson, P D.: Dependency of recrystallization mechanism to the initial grain size 2008, 2830-2840.
<https://ro.uow.edu.au/engpapers/971>

Research Online is the open access institutional repository for the University of Wollongong. For further information contact the UOW Library: research-pubs@uow.edu.au

Dependency of Recrystallization Mechanism to the Initial Grain Size

A. DEGHAN-MANSHADI and P.D. HODGSON

The effect of initial grain size on the recrystallization behavior of a type 304 austenitic stainless steel during and following hot deformation was investigated using hot torsion. The refinement of the initial grain size to 8 μm , compared with an initial grain size of 35 μm , had considerable effects on the dynamic recrystallization (DRX) and post-DRX phenomena. For both DRX and post-DRX, microstructural investigations using electron backscattered diffraction confirmed an interesting transition from conventional (discontinuous) to continuous DRX with a decrease in the initial grain size. Also, there were unexpected effects of initial grain size on DRX and post-DRX grain sizes.

DOI: 10.1007/s11661-008-9656-5

© The Minerals, Metals & Materials Society and ASM International 2008

I. INTRODUCTION

THE objective for thermomechanical processing of steels is generally to improve the final mechanical properties by refining the room-temperature grain size. In the steel industry, this is achieved through austenite conditioning, where the large initial, as cast or reheated, grain size is refined through recrystallization during or after deformation. In structural steels, there is also transformation from austenite to ferrite. Insight into the hot-working behavior of steels is often obtained through the use of alloys that do not transform during quenching to room temperature. This includes the use of conventional stainless steels or Fe-Ni model alloys to study the dynamic and static recrystallization reactions.

The characteristics of dynamic recrystallization (DRX) and post-DRX in austenite at a constant initial grain size and under different deformation conditions have been studied by numerous authors.^[1-8] The initial grain size has a strong influence on the kinetics of recrystallization and microstructure due to the change in the grain-boundary surface area, which is the principal nucleation site. It is well known that in hot deformation, a decrease in the initial grain size will accelerate the onset of DRX, increase DRX kinetics and also affect the microstructural and mechanical characteristics of the deformed structure.^[5,9,10] While for a given deformation condition, the effect of initial grain size on DRX final grain size and steady-state stress is less pronounced, a transition from single- to multiple-peaks behavior is reported in several materials when the initial grain size is decreased below a critical value.^[5,11,12]

Conventional DRX of austenite usually occurs through a discontinuous mechanism, involving nucleation and growth of strain-free grains,^[2,13] *i.e.*, by serration, bulging, and then migration of original high-angle grain boundaries (HAGB). However, under certain test conditions or initial microstructures, a transition from discontinuous recrystallization (DDRX) to continuous recrystallization (CDRX) has been reported in austenite.^[11,14,15] For example, a transition from DDRX to CDRX was observed in 316L austenitic stainless steel with a decrease in the deformation temperature (starting with a similar initial grain size and at similar strain rates).^[15] In other research,^[11] decreasing the initial grain size to a very small value of 2.8 μm in 304 austenitic stainless steel led to a continuous type of DRX based on grain-boundary sliding.

Continuous recrystallization, which also has been termed “rotation recrystallization,” “*in-situ* recrystallization,” or “extended recovery,” is accompanied by a continuous increase in the misorientation of low-angle grain boundaries (LAGB) without (or very limited) migration of HAGB. Such a mechanism is common in the superplastic deformation of some high SFE metals, such as Al alloys,^[16,17] Mg alloys,^[18] and ferritic steels.^[19-21]

The significant effects of initial grain size on the post-DRX recrystallization in different materials has also been reported in a number of studies.^[14,22] For example, it has been shown that during annealing of a deformed Al alloy, a transition from DDRX to CDRX can occur with a considerable decrease in the initial grain size.^[22]

Numerous researchers have studied the DRX and post-DRX behaviors of steels and other alloys, considering the effect of different variables, including temperature, chemical composition, and strain rate.^[1,23-25] However, there are few studies on the influence of initial grain size, particularly for very fine initial grain sizes, on these phenomena. This is of particular interest in rolling processes that aim to

A. DEGHAN-MANSHADI, Research Fellow, is with the Faculty of Engineering, University of Wollongong, NSW, 2522, Australia. P.D. HODGSON, Professor, is with the Centre for Material and Fibre Innovation, Deakin University, Waurn Ponds, VIC, 3217, Australia. Contact e-mail: alidm@uow.edu.au

Manuscript submitted April 21, 2008.

Article published online October 2, 2008

produce very fine grain sizes in the austenite. For example, in hot-strip mills or bar mills, it is possible that very fine grain sizes could be produced between passes, and it is important to understand the effect of this on the subsequent deformation and recrystallization behavior(s). Therefore, the present work aims to study the DRX and post-DRX processes for a very fine initial grain-size material and compare this with a typical coarser initial grain size.

II. EXPERIMENTAL METHODS

A Type 304 austenitic stainless steel with chemical composition (wt pct) of Fe-0.02 pct C-1.6 pct Mn-8.2 pct Ni-18.5 pct Cr-0.8 pct Cu was used in this study. Torsion samples with a gage length of 20 mm and a diameter of 6.7 mm were machined from rolled bars. The detailed description of test equipment and torsion samples has been provided elsewhere.^[26] Hot- (or warm-) torsion tests were carried out under different deformation conditions of temperature and strain rate. A roughing process at 1200 °C was used to achieve a homogenized microstructure. The samples were then cooled at 1 °Cs⁻¹ to 900 °C and held for two minutes, resulting in a homogenized microstructure with an average grain size of 35 μm. To obtain a smaller grain size, the samples were further deformed to a strain of 1.5 at a strain rate of 1 s⁻¹. The deformed samples were then held for 33 seconds at this temperature, resulting in a homogenized microstructure with an average grain size of approximately 8 μm.

From here, the following different deformation processes were performed on the samples with both initial grain sizes of 35 and 8 μm.

- To investigate the deformed microstructure (DRX process), samples were cooled to various deformation temperatures, deformed to different strains at different strain rates, and immediately quenched by water spray.
- To study the postdeformation recrystallized microstructure, the deformed samples were held for different times before quenching.
- To measure the softening fraction, the deformed samples were held for different times and followed by a second twist to a strain of 0.2 or higher (at the same temperature and strain rate as the first deformation).

Metallographic observations were performed on tangential sections at a depth of approximately 100 μm below the gage surface. The microstructure of mechanically polished surfaces were investigated by electron backscattered diffraction (EBSD) under an accelerated voltage of 20 kV, a working distance of 25 mm from the gun, and an aperture size of 60 μm. The EBSD maps were analysed using HKL technology channel 5 (Oxford Instruments HKL, Hobro, Denmark). The linear-intercept method^[27] was used to measure the DRX-grain sizes where the twin boundaries were not counted as grain boundaries. The softening fraction was measured using the offset-stress method.^[8]

III. RESULTS

A. Effect of Initial Grain Size on Dynamic Recrystallization

The initial grain size only slightly affected the general shape of flow curves (Figure 1), although several obvious differences were observed in the detail of these curves. These differences varied with the deformation temperature (Figure 1(a)) or strain rate (Figure 1(b)). While at low temperatures, this effect was negligible (*i.e.*, 700 °C) and increasing the temperature increased this difference. At a deformation temperature of 750 °C, the flow curve of the finer-grain material showed a slight peak followed by a steady state, while the flow stress of the coarse-grain material increased continuously to the steady state, indicating a clear delay in the initiation of DRX. By increasing the temperature to 850 °C or higher, the typical DRX-flow curve was observed for both initial grain sizes but with considerably different peak and critical strains and stresses. As a general trend, the peak stress and strain of the fine-grain material was significantly lower than that of the coarse-grain

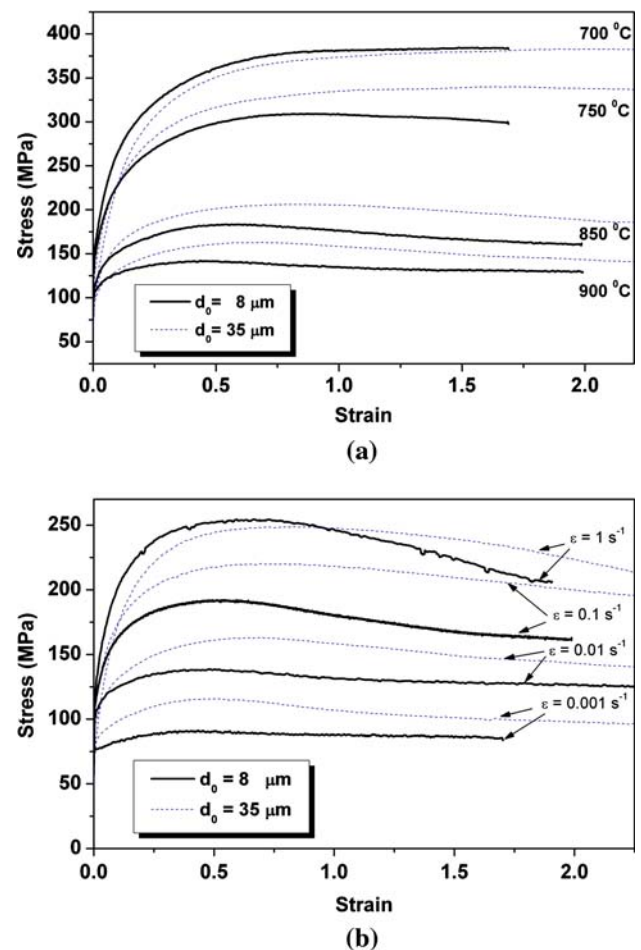


Fig. 1—Flow curves of samples with different initial grain sizes deformed at (a) constant strain rate of 0.01 s⁻¹ and different temperatures and (b) constant temperature of 900 °C and different strain rates.

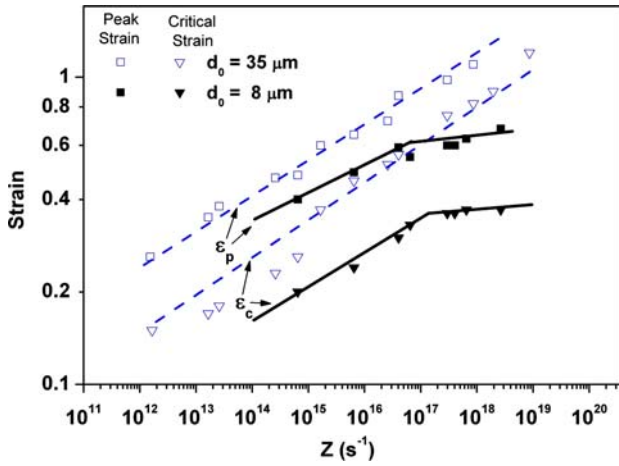


Fig. 2—Peak and critical strains as functions of Z for fine- and coarse-grain materials.

material. This is expected,^[28] whereas the difference in the steady-state stress is usually not reported.^[28,29]

The influence of initial grain size at different strain rates (constant temperature) was similar to the effect of temperature (Figure 1(b)). While the yield stress is often higher for the finer-grain size, the peak and critical strains and stresses decreased noticeably with a decrease in initial grain size, with this effect more pronounced at lower strain rates.

The peak and critical strains showed different relationships with the deformation conditions (*i.e.*, Zener–Hollomon value, Z) in the fine-grain material, compared with the coarse-grain material (Figure 2). While for all Z values, the peak and critical strains of the fine-grain material were lower than for the coarse-grain grains, a slope change was observed in the fine-grain material at a critical Z value (for $Q_{\text{def}} = 400$ kJ/mol) of approximately 10^{17} . Peak and critical strains of the fine-grain material became almost Z independent beyond this critical Z value. On the other hand, the difference between critical and peak strains of fine- and coarse-grain materials decreased with decreasing Z . Overall, though, the ratio of $\varepsilon_p/\varepsilon_c$ was much larger for the fine-grain material (Figure 2).

The effect of initial grain size on peak stress was considerably lower than its effect on peak strain (Figure 3), with no slope change observed in the fine-grain material at high Z values. Figure 3 suggests that the difference between the peak stress of fine- and coarse-grain materials was negligible at very high Z values.

The Z values used in the previous graphs (Figures 2 and 3) had been calculated based on an activation energy (Q) of 400 kJ/mol, previously derived from the flow curves of hot-deformed samples with an initial grain size of $35 \mu\text{m}$.^[7] This value was based on the assumption that the initial grain size has no effect on the flow stress.^[30] However, as observed in Figure 1, the effect of grain size is considerable, and the extent of this effect varies with deformation temperature or strain rate (Figure 3). Therefore, it is possible that the initial grain size will affect the activation energy.

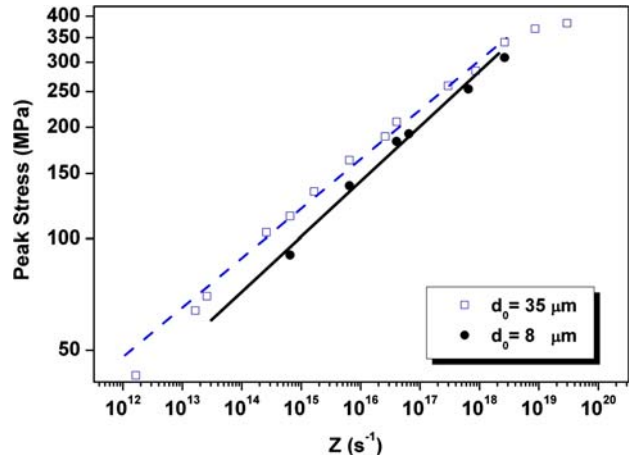


Fig. 3—Peak stress as a function of Z for fine- and coarse-grain materials.

Table I. Activation Energy of Materials with Different Initial Grain Sizes

d_0 (μm)	α	n	Q (kJ/mol)
35	0.0075	5.51	407
8	0.0045	5.15	354

The flow curves and the results of their analysis (peak strain and stress) have been used to estimate the activation energy of hot deformation based on the following equation used by Sellars and Tegart:^[30]

$$Z = A [\sinh(\alpha\sigma)]^n = \dot{\varepsilon} \exp\left(\frac{Q}{RT}\right) \quad [1]$$

where $\dot{\varepsilon}$ is the strain rate (s^{-1}); A , α , and n are constants independent of temperature; σ is the stress (MPa), Q is the hot-deformation activation energy (kJ/mol), R is the gas constant, and T is the absolute temperature (Kelvin). Using linear-regression methods and the value of α , which led to the smallest standard deviation, the values in Table I were found for the preceding equation (based on the procedure explained in Reference 31).

The value of Q for the coarse-grain material (approximately 400 kJ/mol) is in good agreement with the value of activation energy of 304 austenitic stainless steel proposed by others,^[2,25,32] working mostly on materials with an initial grain size of $50 \mu\text{m}$ or above. No value was found for the activation energy of fine-grain austenitic stainless steel in the literature.

Although the reason for the effect of initial grain size on the activation energy is not well understood, one possibility is that different mechanisms (or a range of mechanisms) control hot deformation for the fine and coarse initial grain conditions. If the recrystallization mechanism changes from DDRX to CDRX (or as Belyakov *et al.*^[11] have had proposed to grain-boundary sliding) with decreasing initial grain size, this may explain the change in activation energy. Discontinuous dynamic recrystallization, which is based on the serration and local migration of grain boundaries (bulging),

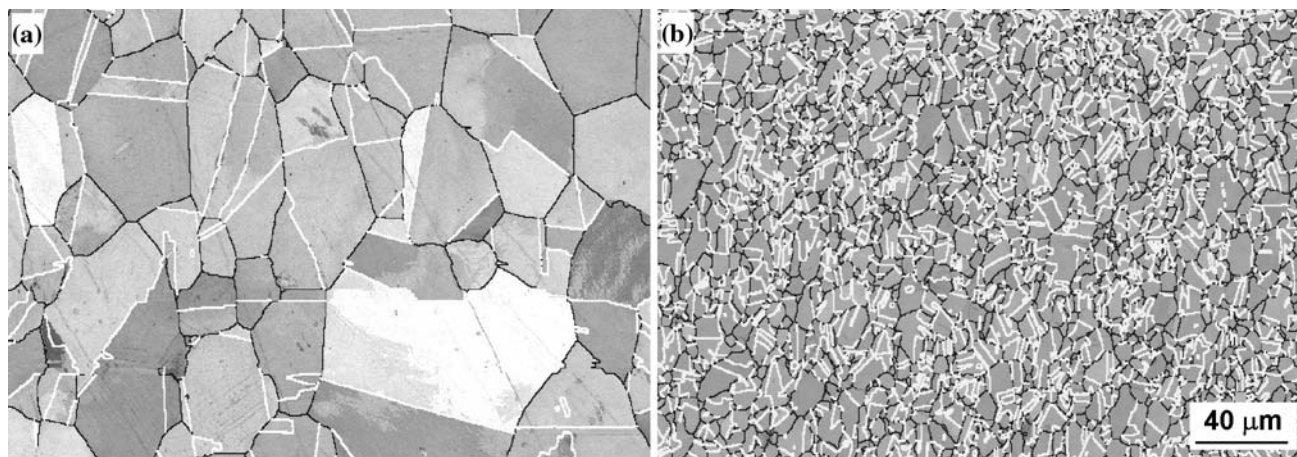


Fig. 4—EBSD maps of initial microstructures (a) $d_0 = 35 \mu\text{m}$ and (b) $d_0 = 8 \mu\text{m}$. High angle ($\theta > 15 \text{ deg}$) and twin boundaries shown by black and white lines, respectively.

needs a different level of energy compared to CDRX, which is based on the increasing misorientation of sub-boundaries. This possibility will be discussed later using the microstructure evidence. A similar effect of initial grain size on the activation energy of a warm-deformed Ti interstitial free steel has been reported by Oudin *et al.*^[29]

The effect of different deformation parameters (at a constant initial grain size of $35 \mu\text{m}$), such as temperature, strain, and strain rate, on the DRX and post-DRX microstructures of this steel were presented in other previous work.^[1,4,6,7] As the initial grain size has a pronounced effect on the evolution of the deformed microstructure, its effect was investigated at a constant deformation temperature of $900 \text{ }^\circ\text{C}$ and a strain rate of 0.01 s^{-1} for the two initial grain sizes.

Both initial microstructures consisted of equiaxed grains with a large quantity of twin boundaries of 50 and 43 pct for the coarse and fine initial microstructures, respectively (Figure 4).

The deformed microstructures at different strains strongly depend on the initial grain size (Figures 5 and 6). Under the present deformation condition, the conventional DRX features, such as grain-boundary serration, bulging of new DRX grains on serrated pre-existing grain boundaries, and formation of necklace structure are observed in the coarse material (Figure 5).

In the fine-grain material, the serration of grain boundaries was less obvious. However, a large quantity of new DRX grains formed on the pre-existing grain boundaries and particularly at the triple junctions (Figure 6(a)). Because the number of triple junctions in the fine-grain material is much higher than for the coarse grain, a large number of new grains were formed at these sites, and, therefore, the necklace structure was less apparent. With increasing strain beyond the peak stress (Figure 6(b)), more new small grains were formed on the pre-existing grain boundaries or within the grains. The final microstructure (Figure 6(d)) consisted of small equiaxed grains which replaced the initial structure.

A comparison between Figures 5 and 6 indicates several differences during the development of the DRX microstructure in both materials.

- The serration of grain boundaries and development of the DRX microstructure based on the necklace structure was observed mostly for the coarse-grain material.
- A fully recrystallized microstructure in the fine-grain material was established at a strain much lower than for the coarse-grain size.
- Intragranular DRX nucleation and also deformation features inside the original grains were only observed in the coarse-grain material.
- The formation of new DRX grains at triple junctions and nonequilibrium grain-boundary junctions (*i.e.*, quadruple junctions) mainly occurred in the fine-grain material.

Apart from the preceding differences, another important difference between the microstructure developed from the fine and coarse initial grains is the formation of substructure and its role in the evolution of DRX. The microstructure developed in the coarse-grain material can be characterized by two types of deformation substructure. The first consisted of a dense cell structure, which mainly appeared adjacent to the initial grain boundaries. The second type included some elongated sub-boundaries with large distances between them. The later type was mainly formed in the grain interior. However, the major part of the substructure in the fine-grain material was from the second type. Figure 7 shows examples of such substructures in both materials. These are the same samples shown in Figures 5(c) and 6(b), respectively.

To gain a better understanding of the influence of the initial grain size on the evolution of microstructure and substructure during hot deformation, the average linear-intercept distances of LAGB (*i.e.*, $l_{1.5}$) and HAGB (*i.e.*, l_{15}) were measured. The average distances of LAGB in the fine-grain material decreased rapidly with increasing strain and reached a steady state (approximately $3 \mu\text{m}$)

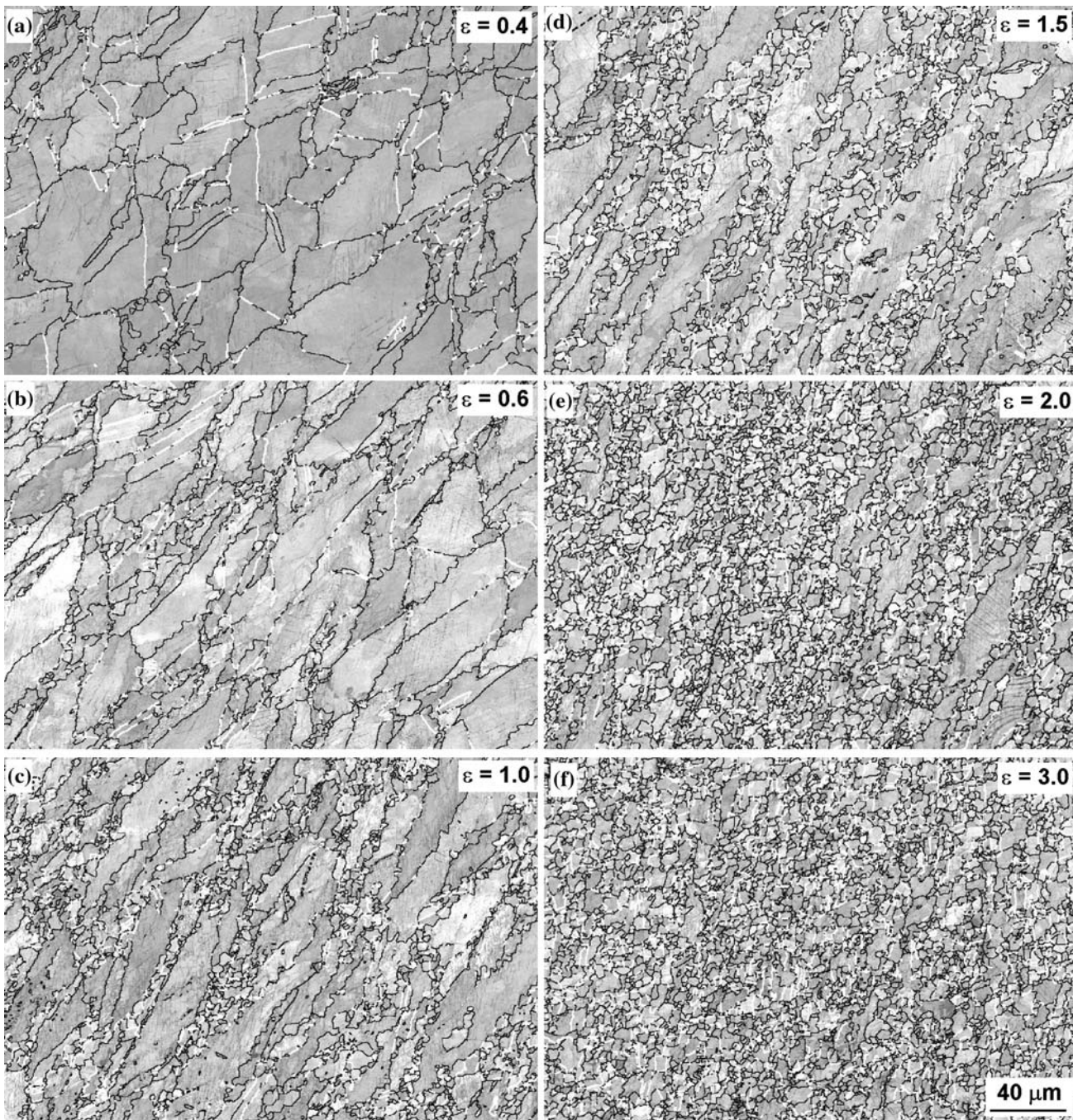


Fig. 5—EBSD maps of the coarse-grain material deformed at 900 °C and a strain rate of 0.01 s⁻¹. High angle ($\theta > 15$ deg) and twin boundaries shown by black and white lines, respectively.

at a strain as low as 0.5. In contrast, this value in the coarse-grain material decreased slowly but reached the nearly same steady-state value at a much higher strain of 1.5 (Figure 8). The linear intercept between HAGB shows a distinctly different dependency to the initial grain size. While the l_{15} in the fine-grain material decreased dramatically with increasing strain and reached a steady-state value of approximately 4 μm at a strain of 1.0, this steady state for coarse-grain material is approximately 6.5 μm at a strain of 2.0 (Figure 9). Therefore, the effect of initial grain size on HAGB

distances (or steady-state grain size) is stronger than on LAGB distances.

The frequency of LAGB, which is superimposed in Figure 8, shows the difference in the substructure evolution during hot deformation for the fine- and coarse-grain materials. While a high quantity of LAGB formed in the coarse-grain material, their frequency in the fine initial grain size is considerably lower. Both curves reached a steady state at high strains. However, this steady state value (*i.e.*, LAGB pct) in the coarse-grain material is almost twice the fine-grain material.

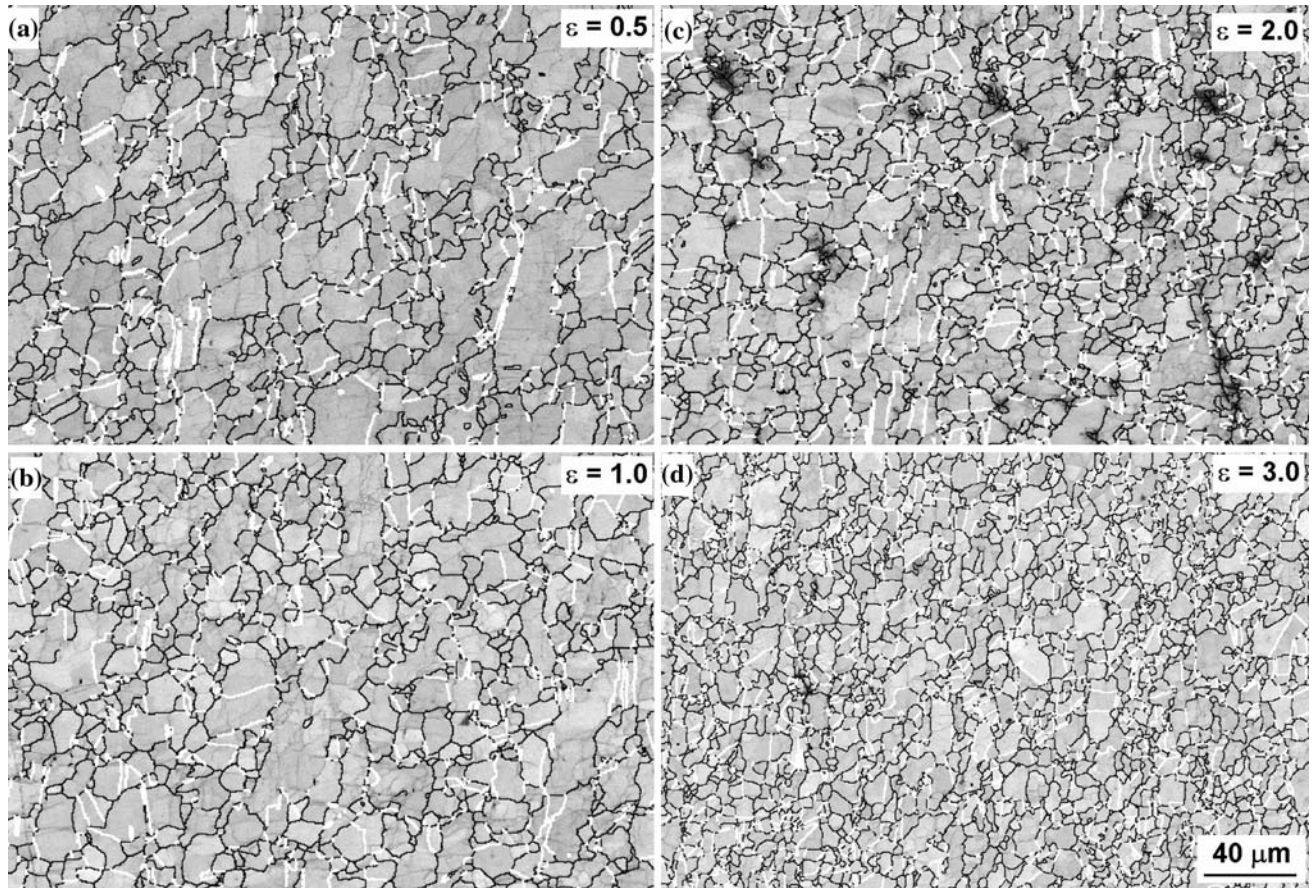


Fig. 6—EBSD maps of the fine-grain material deformed at 900 °C and a strain rate of 0.01 s⁻¹. High angle ($\theta > 15$ deg) and twin boundaries are shown by black and white lines, respectively.

As observed in the flow curves, the critical and peak strains of the fine-grain material are less than the coarse grain, indicating DRX has started earlier than in the coarse-grain material. Figure 10 shows the difference between the DRX kinetics for both materials under a constant deformation condition of 900 °C and 0.01 s⁻¹, which supports that DRX commenced much sooner than in the coarse grain and also has reached a maximum value at a lower strain.

To compare between the kinetics of DRX in both materials and over a wide range of deformation conditions, the Avrami exponent was measured under different deformation conditions (Z values) from the flow-curve analysis. Assuming that the mechanical softening observed on the flow curves is directly related to the DRX volume fraction, the following constitutive equation can give the recrystallized fraction (X) at any strain beyond the initiation point of DRX.^[12]

$$X = \frac{\sigma_s - \sigma}{\sigma_s - \sigma_{ss}} \quad [2]$$

where σ_s is the saturation stress in the absence of DRX, which can be considered as peak stress, and σ_{ss} is the steady-state stress.

Therefore, the Avrami exponent (n) can be determined by plotting the $\ln(\ln(1/(1-X)))$ as a function of \ln

$(\varepsilon - \varepsilon_p)$.^[33] The Avrami exponent was determined at different deformation conditions for both fine- and coarse-grain materials (Figure 11). While the deformation conditions did not show any significant effect on this value, the effect of initial grain size is considerable with the fine-grain material having a higher n value, indicating a higher rate of DRX. The most important reason for the effect of initial grain size on DRX kinetics could be related to the amount and the nature of available nucleation sites. In fact, decreasing the initial grain size will increase the number of grain corners or triple junctions (the best sites for initiation of DRX grains), grain edges, and grain surfaces. Additionally, assuming similar nucleation at the grain edges and grain surfaces (grain boundaries) for a given grain-boundary migration rate, the DRX period will be completed sooner for the fine-grain material.

B. Effect of Initial Grain Size on Postdynamic Recrystallization

The effect of initial grain size on postdynamic recrystallization is reported through its effect on the time for 50 pct softening (Figure 12). The considerable effect of initial grain size on both the strain dependent and independent regions is obvious, even though it is generally accepted that grain size should have no effect

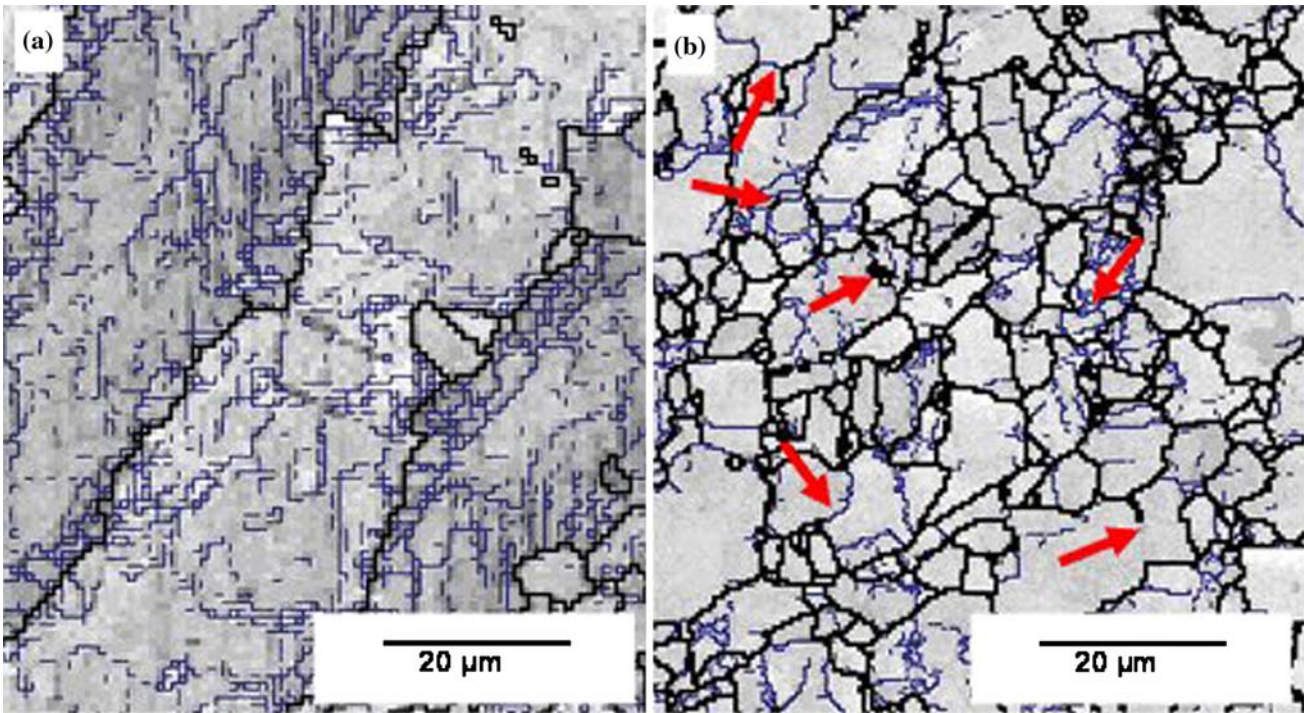


Fig. 7—EBSD maps of samples deformed at 900 °C and a strain rate of 0.01 s^{-1} to a strain of 1.0. (a) Coarse-grain material ($d_0 = 35 \mu\text{m}$) and (b) fine-grain material ($d_0 = 8.0 \mu\text{m}$). Arrows show the incomplete HAGB in the structure. High-angle ($\theta > 15 \text{ deg}$) and low-angle ($\theta > 1.5 \text{ deg}$) boundaries shown by thick and thin lines, respectively.

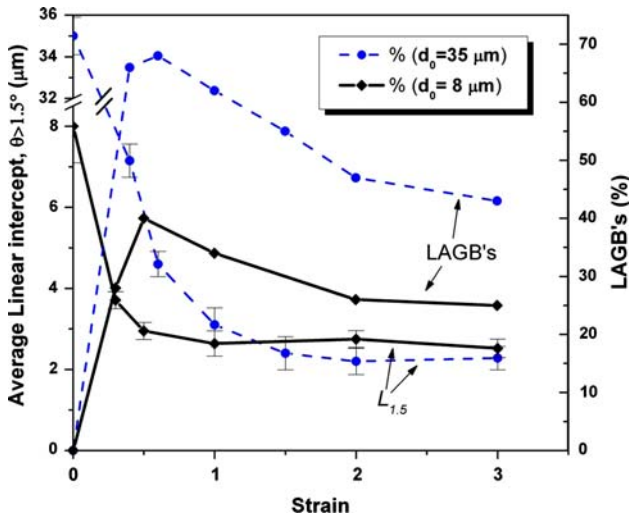


Fig. 8—LAGB and their average linear intercept as functions of strain.

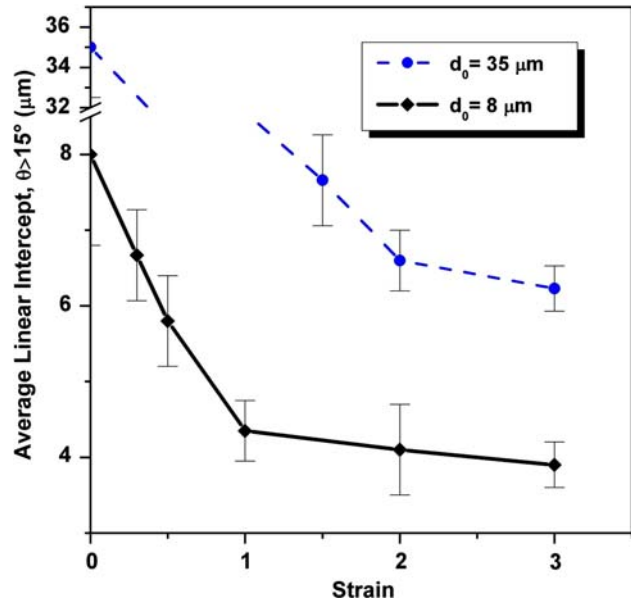


Fig. 9—Average linear intercepts of HAGB as a function of strain.

on the strain-independent region.^[34] However, its influence on the strain-dependent region, where static recrystallization (SRX) is assumed to be the dominant softening mechanism,^[23,35] is stronger than the strain-independent region. The transition strain, ε^* , is also affected by the initial grain size, decreasing with decreasing initial grain size.

Electron backscattered diffraction analysis was performed on both fine and coarse initial grain materials deformed to a strain of 1.0 (at 900 °C and 0.01 s^{-1}) and

held for different times before quenching. A considerable effect of initial grain size was observed on the linear intercept of HAGB during unloading. The normalized average grain size (linear intercept), d/d_0 , during annealing (Figure 13) showed that, while in the fine-grain material, the recrystallized-grain size reached the initial grain size after a short annealing time (approximately

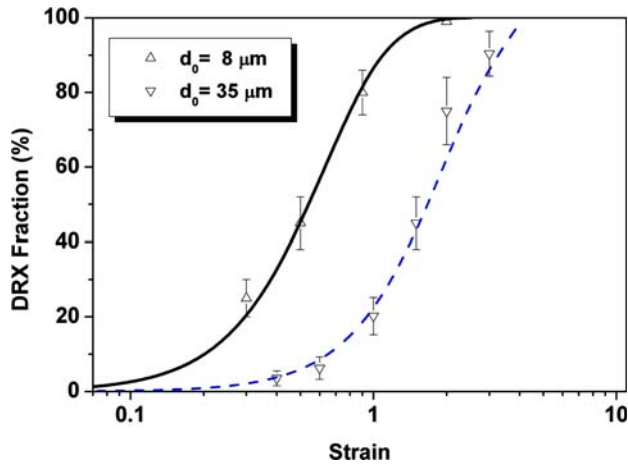


Fig. 10—DRX fraction as a function of strain ($T = 900\text{ }^{\circ}\text{C}$ and $\dot{\epsilon} = 0.01\text{ s}^{-1}$) for fine- and coarse-grain materials.

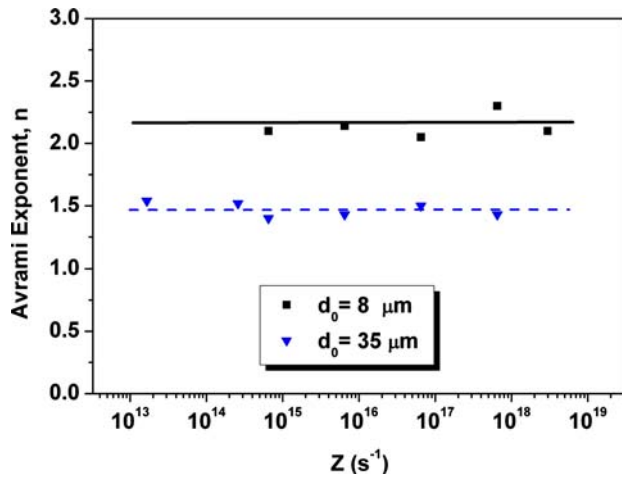


Fig. 11—Avrami exponent as a function of Zener-Hollomon parameter for fine- and coarse-grain materials.

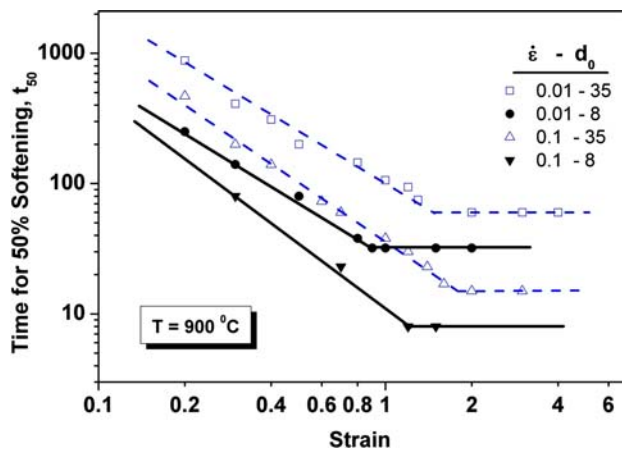


Fig. 12—Time for 50 pct softening as a function of strain.

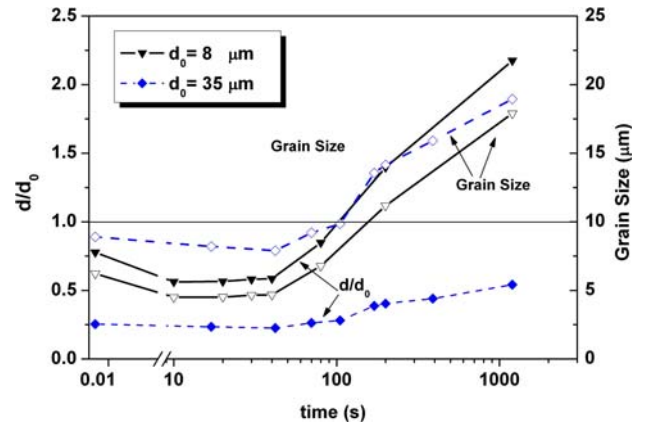


Fig. 13—Normalized (d/d_0) and average grain sizes as functions of unloading time.

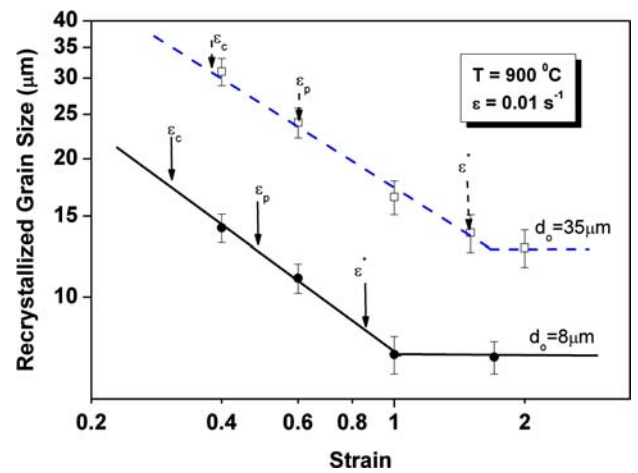


Fig. 14—Postdeformation recrystallized grain size as a function of strain for fine- and coarse-grain materials.

100 seconds) and then grew quickly; in the coarse-grain material, the recrystallization and coarsening rate was much lower, and the recrystallized-grain size could not attain the initial grain size even after annealing for very long times. This indicates the more effective coarsening process after recrystallization of the fine-grain material compared to the coarse-grain one. Interestingly, the final grain sizes (after 1200 seconds of unloading time) in both materials were very similar.

The evolution of the fully recrystallized-grain size as a function of strain (Figure 14) implies that strain is an important variable and, similar to t_{50} , there is a strain-dependent and a strain-independent region with a transition strain. The initial grain size has a great effect on the recrystallized-grain size for both the strain-dependent and independent regions; again no effect is expected in the strain-independent region.^[36] The effect of initial grain size on the strain where the grain-size dependency to the strain changed from strain dependent to strain independent was also significant.

IV. DISCUSSION

The present results imply significant effects of initial grain size on microstructure development during and after hot deformation. In other words, the mechanical properties, the microstructural characteristics, and the kinetics of both DRX and post-DRX clearly depend on the starting microstructure. Generally, it is accepted that grain size will play a major role in the initiation of DRX and the rate of SRX, whereas its effect on DRX and post-DRX is expected to be minor. However, this is clearly not the case in the current work.

One potential reason for an effect of grain size is a change in the DRX mechanism. Previous work on Al alloys,^[16,17] Ni-30Fe,^[37] and stainless steel^[11] have shown occurrence of CDRX in materials with a very small initial grain size. In the present work, there is some evidence to support a change from DDRX to CDRX by the microstructure and substructure analysis of the fine- and coarse-grain materials. The deformed microstructure of the fine-grain material showed that the misorientation of some segments of the substructure network increased during deformation and changed to HAGB (arrows in Figure 7). This type of increase in the misorientation of LAGB inside the deformed grains is consistent with the CDRX model proposed by Gourdet and Montheillet.^[38] Therefore, CDRX can be considered as an alternative mechanism acting together with the conventional DRX in the fine-grain materials. On the other hand, as mentioned previously, the formation of DRX grains at triple junctions and nonequilibrium grain-boundary junctions (*i.e.*, quadruple junctions) in the fine-grain material suggests the formation of these grains by the grain-boundary sliding mechanism.^[39] Nevertheless, some new DRX grains were also formed based on the bulging of initial grain boundaries in fine-grain material.

An important microstructural parameter that can affect the recrystallization during hot deformation of fine and coarse initial grain materials is the number of triple junctions. As the number of these junctions, which are highly favorable sites for nucleation of DRX grains,^[39,40] is very high in the fine-grain materials, the nucleation of DRX grains can start at lower strains on these junctions (it does not need the initial grain boundaries to serrate). For example, it has been mathematically shown^[12] that the number of nucleation sites (for a nucleus with a 1- μm diameter) at triple junctions for a material with an initial grain size of 8 μm is almost 20 times more than for an initial grain size of 35 μm . The formation of a DRX grain on these junctions can also change the DRX structure from a necklace to a homogeneously distributed structure (Figure 6). According to Miura *et al.*,^[41] grain-boundary sliding is the most probable mechanism for nucleation at these triple junctions.

The difference in the DRX process in the fine- and coarse-grain materials can be traced through the different effect of deformation on sub-boundary ($\theta < 15$ deg) and boundary ($\theta > 15$ deg) evolution during hot deformation. Comparison between Figures 8 and 9 shows that the difference between the average linear intercept

of low- ($l_{1.5}$) and high- (l_{15}) angle grain boundaries in the fine-grain material is less than the coarse-grain material. This demonstrates that a DRX mechanism based on the coalescence of sub-boundaries (*i.e.*, CDRX) can play an important role in the progress of DRX for the fine-grain material. On the other hand, the low sensitivity of l_{15} in the fine-grain material to strain (at strains higher than 1.0) suggests that a mechanism based on the rearrangement of HAGB, such as grain-boundary sliding, may be responsible for DRX of samples deformed at any strain higher than 1.0. In the coarse-grain material, the insensitivity of average linear intercept to the strain occurred at a strain much higher than the fine-grain material.

The difference in the DRX mechanism of fine- and coarse-grain materials also caused a moderate effect on the recrystallized-grain size. This is somewhat in contrast to other work, with reports of no effect of initial grain size on the DRX-grain size.^[5,11,42] Figure 15 shows the dependency of the DRX-grain size on the initial grain size as a function of Z . For comparison, the DRX-grain size observed by hot deformation of an ultrafine-grain size (2.8 μm) austenitic stainless steel^[11] has been superimposed to this figure. This ultrafine-grain structure was developed by multiple warm compression while decreasing the temperature from 950 $^{\circ}\text{C}$ to 600 $^{\circ}\text{C}$ (50 $^{\circ}\text{C}$ at each pass).^[43] These small grains were formed through CDRX under warm-deformation conditions and static recovery (and grain growth) during heating to the next pass.^[11] As is clear in Figure 15, there is a dependency of DRX-grain size to the initial grain size, and this dependency increases with decreasing initial grain size. However, no noticeable dependency was observed for initial grain sizes larger than 35 μm .^[1,44] One logical explanation for this effect is the difference in the DRX mechanisms for the different initial grain sizes noted previously. It is reasonable to expect a difference between the grain size of a discontinuously recrystallized microstructure (evolved based on the local migration of grain boundaries) and a continuously recrystallized microstructure (evolved based on the coalescence of subgrains).

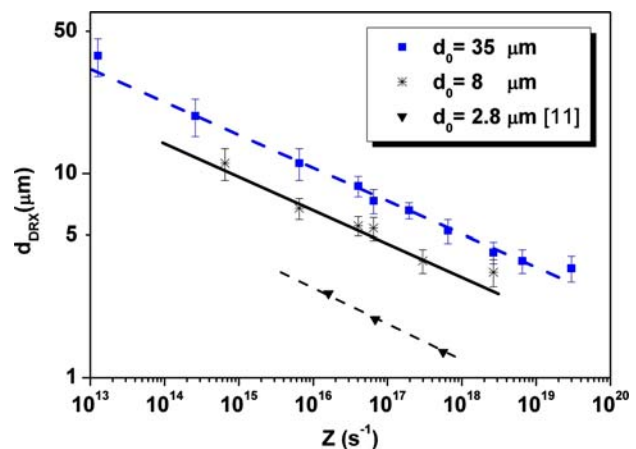


Fig. 15—DRX grain size as a function of Z .

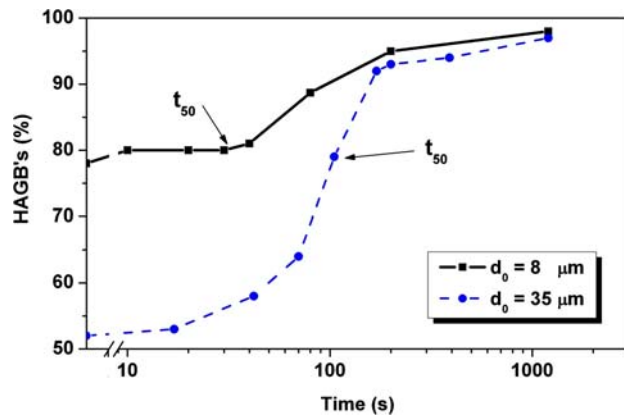


Fig. 16—Frequency of HAGB as a function of unloading time.

Grain growth may play another role for the finer-grain size in CDRX compared with DDRX. When CDRX is involved, experimental results have shown that the migration rate of HAGB is almost three orders of magnitude smaller than when DDRX is involved.^[45,46] Therefore, it can be expected that the grain growth is limited where CDRX is dominant, and the grain size becomes finer than DDRX.

The preceding discussion implies that while in coarse-grain material, the conventional DRX, *i.e.*, the serration and bulging of pre-existing grain boundaries, is the dominant restoration mechanism, a mix of conventional and CDRX, as well as grain-boundary sliding operates as the restoration mechanism in the fine initial grain materials. On the other hand, a comparison between the present results and other relevant work^[11,16,44,47] suggests a mechanism transfer from conventional DRX (DDRX) to CDRX and then to grain-boundary sliding with a decrease in the initial grain size. However, a wide overlap area between the different mechanisms is possible.

A. Effect of Initial Grain Size on Postdynamic Recrystallization

The effect of initial grain size on t_{50} in the strain-dependent region, where static recrystallization is the most important softening mechanism,^[35] is expected. Because the grain boundaries are the sites for initiation of SRX grains and the number of these sites in the fine initial grain material is much higher than the coarse-grain one, the rate of recrystallization should be higher. However, in the strain-independent region, where the post-DRX is the most important restoration mechanism,^[35] there should not be any major dependency on the initial grain size, at least whenever a similar mechanism is the responsible for recrystallization.

Similar to DRX, the change in the mechanism of recrystallization can be considered as a possible reason for such an effect of the initial grain size on post-DRX kinetics. Belyakov *et al.*^[14] have shown that, unlike the coarse initial grain size, the recrystallization process during the annealing of a very fine grain size 304 stainless steel is continuous, followed by a normal grain

growth. The same transition from discontinuous to continuous static recrystallization with a decrease in the initial grain size has also been reported for some Al alloys.^[22]

In the present work, the transition between DDRX and CDRX during the unloading can be monitored by EBSD analysis. The change in the frequency of HAGB represents a very reliable method to identify the nature of the recrystallization process during annealing.^[22,48] Based on this hypothesis, when the recrystallization mechanism is discontinuous, there is a relatively sharp increase in the frequency of HAGB. This is due to the quick consumption of deformed substructure by recrystallizing grains, and, therefore, a major decrease in LAGB frequency. On the other hand, when CDRX occurs, there is little change in the frequency of HAGB.

Figure 16 shows a sharp increase in the frequency of HAGB with increasing annealing time in the coarse-grain material. However, in the fine-grain material, this sharp slope does not exist. Figure 16 shows that while there is no obvious change in the HAGB frequency in the fine-grain material, more than 50 pct mechanical softening (t_{50}) has occurred in this material. However, in the coarse-grain material, 50 pct softening was accompanied with a large increase in the HAGB frequency. The EBSD analysis implied that 50 pct softening in the fine-grain material can mainly be through the growth of recrystallized grains (Figure 13). However, static recovery (prior to CDRX) can also be considered as a restoration mechanism in this material.

The preceding considerations suggest that CDRX is an important mechanism for postdynamic softening in the fine initial grain material.

V. CONCLUSIONS

The effect of initial grain size on recrystallization during and following hot deformation of austenite was examined using a 304 austenitic stainless steel in torsion. The main points raised from this study are as follows.

1. As expected, the peak and critical strains decreased with initial grain size and followed a power-law function with the Zener–Hollomon parameter. However, at a critical value (Z approximately 10^{17}), the finer-grain size showed almost no change with increasing Z ; for the coarse-grain size, there was no change in behavior over the entire Z range.
2. The activation energy for hot working changed from 407 to 354 kJ/mol for the coarse- and fine-grain materials, respectively.
3. Contrary to most work where the dynamic grain size is independent of the initial grain size, decreasing the initial grain size to the very low value of $8 \mu\text{m}$ led to a finer dynamic grain size. It also increased the recrystallization kinetics after deformation, most importantly, in the strain-independent regime which has again been previously thought to be insensitive to initial grain size.
4. There was evidence that the fine initial grain size promoted CDRX.

5. The Avrami exponent, n , in the fine-grain material was almost 1.5 times greater than the coarse-grain material.

REFERENCES

1. A. Dehghan-Manshadi, M.R. Barnett, and P.D. Hodgson: *Mater. Sci. Eng. A*, 2008, vol. 458, pp. 664–72.
2. A. Belyakov, H. Miura, and T. Sakai: *Mater. Sci. Eng. A*, 1998, vol. 255, pp. 139–47.
3. C.M. Sellars: in *Hot Working and Forming Process*, C.M. Sellars and C.H.J. Davies, eds., TMS, Warrendale, PA, 1979, pp. 3–15.
4. A. Dehghan-Manshadi, H. Beladi, M.R. Barnett, and P.D. Hodgson: *Mater. Forum*, 2004, vols. 467–470, pp. 1163–68.
5. T. Sakai and J.J. Jonas: *Acta Metall.*, 1984, vol. 32, pp. 189–209.
6. A. Dehghan-Manshadi and P.D. Hodgson: *ISIJ Int.*, 2007, vol. 47, pp. 1799–1803.
7. A. Dehghan-Manshadi, M.R. Barnett, and P.D. Hodgson: *Metall. Mater. Trans. A*, 2008, vol. 31A, pp. 1359–70.
8. A. Dehghan-Manshadi, M.R. Barnett, and M.A. Hodgson: *Metall. Mater. Trans. A*, 2008, vol. 39A, pp. 1371–81.
9. P.J. Wray: *Metall. Trans. A*, 1984, vol. 15A, pp. 2009–19.
10. P.J. Wray: *Metall. Trans. A*, 1975, vol. 6A, pp. 1197–1203.
11. A. Belyakov, H. Miura, and T. Sakai: *Scripta Mater.*, 2000, vol. 43, pp. 21–26.
12. M. El Wahabi, L. Gavard, F. Montheillet, J.M. Cabrera, and J.M. Prado: *Acta Mater.*, 2005, vol. 53, pp. 4605–12.
13. F.J. Humphreys and M. Hatherly: *Recrystallization and Related Annealing Phenomena*, 1st ed., Pergamon Press, Oxford, United Kingdom, 1996.
14. A. Belyakov, T. Sakai, H. Miura, R. Kaibyshev, and K. Tsuzaki: *Acta Mater.*, 2002, vol. 50, pp. 1547–57.
15. C. Donadille, C. Rossard, and B. Thomas: in *Annealing Processes—Recovery, Recrystallization, and Grain Growth*, 7th Risø Int. Symp. Metallurgy and Materials Science, N. Hansen, D. Jull Jensen, T. Leffers, and B. Ralph, eds., Risø National Laboratory, Roskilde, Denmark, 1986, pp. 285–90.
16. H. Jazaeri and F.J. Humphreys: *Acta Mater.*, 2004, vol. 52, pp. 3239–50.
17. H. Jazaeri and F.J. Humphreys: *Mater. Sci. Forum*, 2002, vols. 396–402, pp. 551–56.
18. A. Galeyev, R. Kaibyshev, and T. Sakai: *Mater. Sci. Forum*, 2003, vols. 419–422, pp. 509–14.
19. A. Belyakov, Y. Kimura, and K. Tsuzaki: *Mater. Sci. Eng. A*, 2005, vol. 403, pp. 249–59.
20. P. Cizek, V. Safek, and V. Cerny: *Hutnicke Listy*, 1989, vol. 43, pp. 99–106.
21. F. Gao, Y. Xu, and K. Xia: *Metall. Mater. Trans. A*, 2000, vol. 31A, pp. 21–27.
22. H. Jazaeri and F.J. Humphreys: *Acta Mater.*, 2004, vol. 52, pp. 3251–62.
23. C. Roucoules, P.D. Hodgson, S. Yue, and J.J. Jonas: *Metall. Mater. Trans. A*, 1994, vol. 25A, pp. 389–400.
24. A. Najafi-Zadeh, J.J. Jonas, G.R. Stewart, and E.I. Poliak: *Metall. Mater. Trans. A*, 2006, vol. 36A, pp. 1899–1906.
25. N.D. Ryan and H.J. McQueen: *Can. Metall. Q.*, 1990, vol. 29, pp. 147–62.
26. P.D. Hodgson, D.C. Collinson, and B. Perrett: in *7th Int. Symp. Physical Simulation*, H.G. Suzuki, T. Sakai, and F. Matsuda, eds., NRIM, Tsukuba, Japan, 1997, pp. 219–29.
27. R.L. Higginson and C.M. Sellars: *Worked Examples in Quantitative Metallography*, Maney Publishing, London, 2003, pp. 16–22.
28. J.P. Sah, C.J. Richardson, and C.M. Sellars: *Met. Sci.*, 1974, vol. 8, pp. 325–31.
29. A. Oudin, M.R. Barnett, and P.D. Hodgson: *Mater. Sci. Eng. A*, 2004, vol. 367, pp. 282–94.
30. C.M. Sellars and W.J. McTegart: *Acta Metall.*, 1966, vol. 14, pp. 1136–38.
31. J.L. Uvira and J.J. Jonas: *Trans. Metall. Soc. AIME*, 1968, vol. 242, pp. 1619–26.
32. S.I. Kim and Y.C. Yoo: *Mater. Sci. Eng. A*, 2001, vol. 311, pp. 108–13.
33. W. Roberts, H. Benden, and B. Alben: *Metals Sci.*, 1979, vol. 13, pp. 195–203.
34. W.P. Sun and E.B. Hawbolt: *ISIJ Int.*, 1997, vol. 37, pp. 1000–09.
35. S. Zahiri and P.D. Hodgson: *Mater. Sci. Technol.*, 2004, vol. 20, pp. 456–64.
36. C.M. Sellars: in *J.J. Jonas Symp., Thermomechanical Processing of Steel*, S. Yue and E. Es-Sadiqi, eds., TMS, Warrendale, PA, 2000, pp. 3–19.
37. D.W. Suh, J.Y. Cho, and K. Nagai: *Metall. Mater. Trans. A*, 2004, vol. 35A, pp. 3399–3408.
38. S. Gourdet and F. Montheillet: *Acta Mater.*, 2003, vol. 51, pp. 2658–99.
39. H. Miura, T. Sakai, H. Hamji, and J.J. Jonas: *Scripta Mater.*, 2004, vol. 50, pp. 65–69.
40. S. Andiarwanto, H. Miura, and T. Sakai: *Mater. Sci. Forum*, 2002, vols. 408–412, pp. 761–66.
41. H. Miura, H. Hamji, and T. Sakai: *Mater. Sci. Forum*, 2002, vols. 408–412, pp. 755–60.
42. T. Maki, K. Akasaka, and I. Tamura: in *Thermomechanical Processing of Microalloyed Austenite*, A.J. DeArdo, G.A. Ratz, and P.J. Wray, eds., TMS-AIMS, Pittsburgh, 1982, pp. 217–34.
43. A. Belyakov, T. Sakai, H. Miura, and R. Kaibyshev: *ISIJ Int.*, 1999, vol. 39, pp. 592–99.
44. I. Salvatori, T. Inoue, and K. Nagai: *ISIJ Int.*, 2002, vol. 42, pp. 744–50.
45. S. Gourdet and F. Montheillet: *Acta Mater.*, 2002, vol. 50, pp. 2801–12.
46. A. Belyakov, K. Tsuzaki, H. Miura, and T. Sakai: *Acta Mater.*, 2003, vol. 51, pp. 847–61.
47. T. Sakai, A. Belyakov, and H. Miura: in *1st Joint Int. Conf. Recrystallization and Grain Growth*, G. Gottstein and D.A. Molodov, eds., Springer-Verlag, New York, NY, 2001, pp. 669–82.
48. H. Jazaeri and F.J. Humphreys: *J. Microsc.*, 2004, vol. 213, pp. 241–46.